



QUANTIFYING EARTHQUAKE-INDUCED SOIL NONLINEARITY AND ITS INFLUENCES

Ray Ruichong ZHANG^{1,*}, Stephen HARTZELL², Jianwen LIANG³, and Yuxian HU⁴

SUMMARY

This paper proposes to use a method of nonstationary data processing and analysis, namely the Hilbert-Huang transform (HHT), to characterize earthquake-induced soil nonlinearity and subsequently quantify the influences in seismic site amplification. With the Fourier-based studies as a reference, this study examines the recordings from 2001 Nisqually earthquake and shows that the HHT-based approach is effective and accurate in quantifying soil nonlinearity and its influences in terms of frequency downshift, amplitude-reduction factor, damping-increase factor, and site-amplification factor.

INTRODUCTION

Quantifying influences of soil nonlinearity and/or liquefaction in top soil layer(s) in earthquake ground motion recordings plays an important role in studies of site amplification and liquefaction (e.g., [1]). It could help map accurate seismic hazards in urban areas (e.g., [2]) and design cost-effective geotechnical and structural engineering systems on soils and prone-liquefaction areas (e.g., [3]).

The influences of soil nonlinearity shown in recordings are typically discerned and analyzed with the use of Fourier spectral analysis of the recordings or simply Fourier-based approach. Consensus has been building that the site-amplification factors in the current codes overemphasize the extent of soil nonlinearity, and thus potentially underestimate the level of site amplification. This aspect is demonstrated in [4] that the recording-based site-amplification factors are larger than those in codes for a certain range of base acceleration intensity. In addition, some features of site-amplification factors used in codes and guidance for structural design contradict recent findings from the 1994 Northridge ground motion data set [5]. Since seismic ground motion recordings with liquefaction in the soil layers near the surface typically show similar, but strong nonlinear features of those with soil nonlinearity, the aforementioned consensus and findings will also be applicable to the Fourier-based characterization of liquefaction.

¹ Associate Professor, Division of Engineering, Colorado School of Mines, Golden, CO 80401, USA, Phone: 303-273-3671, Fax: 303-273-3602, Email: rzhang@mines.edu

² Geophysicist, U.S. Geological Survey, MS 966, Box 25046, Denver, CO 80225, USA

³ Professor, Department of Civil Engineering, Tianjin University, Tianjin 300072, China

⁴ Professor, Institute of Geophysics, China Seismological Bureau, Beijing 100081, China

The aforementioned problem might be partly because seismologists and engineers lack sufficient understanding of the underlying causes in nonlinearity. For example, the influence of soil heterogeneity does not scale linearly even when the soil is perfectly linear [6]. In other words, a linear elastic medium with random heterogeneity can change ground motion in a way similar to that caused by medium nonlinearity. Consequently, it is possible for one to interpret the motion influenced by random heterogeneous media as soil nonlinearity (e.g., in the form of damping [7]), which can distort the quantification of site amplification. The problem may also partly because there is lack of an effective approach to properly characterize nonlinearity-induced nonstationary features of ground motion in recordings and then to quantify them.

The objective of this study is to propose the use of a method for nonstationary data processing [8] to characterize and quantify soil nonlinearity and liquefaction from and its influences in earthquake ground recordings.

SIGNATURE OF SOIL NONLINEARITY AND LIQUEFACTION

In general, the stress-strain relationship of a soil becomes nonlinear and hysteretic for a large-amplitude input excitation. Such nonlinearity and hysteresis corresponds to a reduction of soil strength and increased soil damping (e.g., [9-10]).

With a reduction of soil strength such as shear modulus (G) for nonlinear soil, the shear-wave velocity ($v=(G/\rho)^{1/2}$, where ρ is the soil density) and thus the fundamental resonant frequency ($f=v/4h$) of the soil layer with thickness h decreases. Therefore, seismic ground motion recordings over a nonlinear soil layer could show strong wave response at a lower resonant frequency than for the same, but linear layer. Accordingly, increased site amplification at the downshifted soil resonant frequency can be regarded as a signature of soil nonlinearity observable in ground motion records (e.g., [11-12]).

On the other hand, increased damping for nonlinear soil will decrease ground motion, thus moderating the site amplification. Since soil damping is typically frequency dependent, so is the change of damping for nonlinear soil. The increased damping of nonlinear soil is likely lower at higher frequencies [13-14]. The increased site amplification at the downshifted soil resonant frequency and the frequency-dependent increased damping implies that the change in site amplification due to soil nonlinearity should be strongly dependent upon frequency.

Liquefaction is the phenomena of seismic generation of large pore-water pressures and consequent softening of granular soils (e.g., [15]). Therefore, the influences of liquefaction in earthquake ground motion will be similar to those of soil nonlinearity. Accordingly, almost all the aforementioned nonlinear features will also show up in the recordings with liquefaction. Because of the commonality in recordings, this paper refers to site nonlinearity or simply the nonlinearity as the nonlinear phenomena in recordings caused by soil nonlinearity and/or liquefaction.

FOURIER-BASED APPROACH FOR CHARACTERIZING NONLINEARITY

In practice, Fourier series expansion is typically used for representing and analyzing recorded digital data of earthquake ground acceleration $X(t)$, i.e.,

$$X(t) = \Re \sum_{j=1}^N A_j e^{i\Omega_j t} = \Re \sum_{j=1}^N [A_j \sin(\Omega_j t) + iA_j \cos(\Omega_j t)], \quad F(\Omega) = \sum_{j=1}^N |A_j| \quad (1,2)$$

where \Re denotes the real part of the value to be calculated, $i = \sqrt{-1}$ is an imaginary unit, amplitudes A_j are a function of time-independent frequency Ω_j that is defined over the window length T of the data analyzed, j is associated with j -th Fourier component, and F is Fourier amplitude spectrum.

To apply the above Fourier spectral analysis for exploring and thus estimating the influences of site nonlinearity from the seismic ground acceleration at soil site or simply site amplification, two sets of recordings for mainshock and aftershock are typically needed [16], i.e., one at a soil site and the other at a reference site such as bedrock or outcrop. The Fourier spectral ratio for site amplification, referred to as Fourier-based site-amplification factor (FF) here, for an earthquake event (either mainshock or aftershock) can then be found by

$$FF_s(\Omega) = \sqrt{F_{s,h1}^2 + F_{s,h2}^2} / \sqrt{F_{r,h1}^2 + F_{r,h2}^2} \quad (3)$$

where subscripts s and r denote respectively the soil and reference sites, and subscripts $h1$ and $h2$ denote the two horizontal components. Note that Eq. (3) is one of many representatives for site-amplification factor that can be the ratio of characteristics of seismic waves or spectral responses at a site versus reference site.

Since the wave paths and earth structures excluding the soil layer(s) near the surface are almost the same for the soil and reference sites, the site-amplification factor in Eq. (3) eliminates the influences of source from the earthquake event and thus provides the dynamic characteristics of the site. In addition, the recordings at the reference site are generally believed as the results of linear wave responses and the recordings at the soil site subject to the large-magnitude mainshock, but not to the small-magnitude aftershock, are the results of nonlinear wave responses. Accordingly, comparing the site-amplification factors from the mainshock and the aftershock could help explore and quantify the site nonlinearity.

While the above Fourier-based approach or similar methods are widely used, they have, however, the following deficiencies in characterizing the nonstationarity of the earthquake ground motion. Fourier amplitude spectrum defines harmonic components globally and thus yields average characteristics over the entire duration of the data under investigation. While the use of windowed (or short-time) Fourier transform together with Eq. (3) may possibly minimize the nonstationarity in the recordings caused by different types of propagating waves and sources, it also reduces frequency resolution as the length of the window shortens. Thus, one is faced with a trade-off. The shorter the window, the better the temporal localization of the Fourier amplitude spectrum, but the poorer the frequency resolution, which directly influences the measurement of downshift of soil resonant frequency that typically arises in a low-to-intermediate frequency band.

More important, Fourier-based approach cannot resolve the issues of nonstationarity rooted in the nonlinearity. This can be seen from a hypothetical wave record $y(t) = y_1(t) + y_2(t)$, where nonlinear damped response $y_1(t) = \cos[2\pi t + \varepsilon \sin(2\pi t)]e^{-0.2t}$ has time-dependent frequency of $1 + \varepsilon \cos(2\pi t)$ Hz with ε denoting a small factor, and linear response $y_2(t) = 0.05 \sin(30\pi t)$ has constant or time-independent frequency of 15 Hz. The nonlinear response can be expanded into and thus interpreted by a series of linear responses with time-independent frequency, as done by the Fourier spectral analysis. For example, $y(t)$, or $y_1(t)$ in particular, can be interpreted as to contain Fourier components at all frequencies (see Eq. (1) and Fig. 1). Alternatively, Taylor expansion of $y_1(t) \approx [-0.5\varepsilon + \cos(2\pi t) + 0.5\varepsilon \cos(4\pi t)]e^{-0.2t}$, for $\varepsilon \ll 1$, suggests that Fourier transform of $y_1(t)$ consists primarily of two harmonic functions at 1 and 2 Hz respectively, and the width of these two harmonic functions in Fourier amplitude spectrum is proportional to the exponential parameter 0.2 that is

related to damping factor. Note that Fig. 1 uses $\epsilon=0.5$ that is not a small number in comparison with unit and thus shows the third observable peak at 3 Hz in the Fourier amplitude spectrum. Therefore, one can equally well describe $y_1(t)$ by saying that it consists of just two frequency components for $\epsilon \ll 1$, each component having a time varying amplitude that is proportional to $e^{-0.2t}$. The above Fourier-based analysis or interpretation can also be seen in [17-18], among others.

Because the true frequency content of the nonlinear response $y_1(t)$ is bounded between $1-\epsilon$ and $1+\epsilon$, much less than 2 Hz, analysis of the above record suggests that Fourier spectral analysis typically needs higher-frequency harmonic functions (at least 2 Hz for $\epsilon \ll 1$) to simulate the nonlinear data. Stated differently, Fourier spectral analysis distorts the nonlinearity-related nonstationary data. As a result, Fourier-based approach in Eq. (3) will twist the nonlinear site amplification. Similar assertions are confirmed in [19-20], among others, with the aid of solution to classic nonlinear systems such as the Duffing equation.

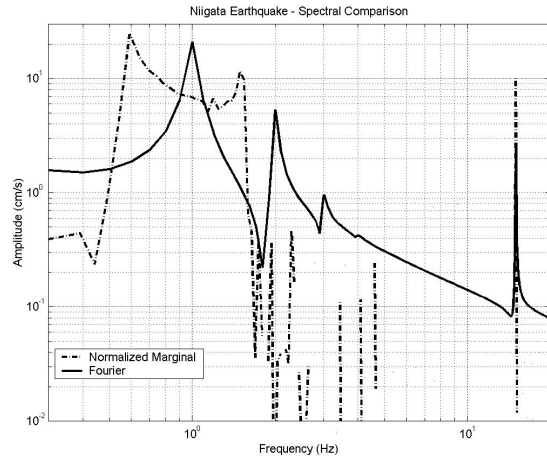


Fig. 1: *Fourier and marginal Hilbert amplitude spectra of a hypothetical record with $\epsilon=0.5$.*

In theory, Fourier spectral analysis in general, or Fourier-based approach for site amplification in particular, can be further used for evaluating damping factor or ratio. For example, the resonant amplification method or half-power, band-width method uses the amplitude change or width of a peak at a certain frequency in the Fourier amplitude spectrum to find the damping factor of a dynamic system (e.g., [21]). However, the distorted Fourier amplitude spectrum for nonlinearity-related nonstationary data will mislead the subsequent use for damping evaluation with site nonlinearity. For example, evaluating the damping ratios at the first and second peaks in the Fourier amplitude spectrum in Fig. 1 suggests that the damping is associated with frequencies at 1 and 2 Hz. In fact, the damping of the record is only dependent on the true frequency content of the nonlinear response $y_1(t)$ bounded between $1-\epsilon$ and $1+\epsilon$, or 0.5 and 1.5 Hz for $\epsilon=0.5$ in Fig. 1. Accordingly, Fourier-based approach would misrepresent the influences of damping as it relates to a nonlinear dynamic system. In addition, Fourier-based damping assessment is typically applicable to a dynamic system with small damping ratio and clearly separate resonant frequencies, which is not the case for the soil layer(s) under investigation.

HHT-BASED APPROACH FOR CHARACTERIZING NONLINEARITY

A method for nonstationary data processing [8] can be used as an alternative to the Fourier-based approach for characterizing site nonlinearity. The method, referred to as Hilbert-Huang transform (HHT), consists of Empirical Mode Decomposition (EMD) and Hilbert Spectral Analysis (HSA). Any complicated time domain record can be decomposed via EMD into a finite, often small, number of intrinsic mode functions (IMF) that admit a well-behaved Hilbert transform. An IMF represents a simple oscillatory mode similar to a component in the Fourier-based sinusoidal function, but more general. The EMD explores temporal variation in the characteristic time scale of the data and thus is adaptive to nonstationary data processes. The HSA defines an instantaneous or time-dependent frequency of the data via Hilbert transformation of each IMF component. The confidence limit of these two unique features is further examined recently in [22], enabling the HHT method more robust and reliable in analysis of

nonstationary data in general and to reveal a possible enhanced interpretive value, alternative to Fourier components and amplitude spectra in particular.

The HHT representation of data $X(t)$ is

$$X(t) = \Re \sum_{j=1}^n a_j(t) e^{i\theta_j(t)} = \Re \sum_{j=1}^n [C_j(t) + iY_j(t)] \quad , \quad \omega_j(t) = d\theta_j(t) / dt \quad (4,5)$$

where $C_j(t)$ and $Y_j(t)$ are respectively the j -th IMF component of $X(t)$ and its Hilbert transform

$$Y_j(t) = \frac{1}{\pi} P \int \frac{C_j(t')}{t-t'} dt' \quad \text{with } P \text{ denoting the Cauchy principal value, and the time-dependent amplitudes}$$

$a_j(t)$ and phases $\theta_j(t)$ are the polar-coordinate expression of Cartesian-coordinate expression of $C_j(t)$ and $Y_j(t)$, from which the instantaneous frequency is defined in Eq. (5). Similar to Fourier series expansion in Eq. (1), Eqs. (4) and (5) indicate that the amplitudes $a_j(t)$ are associated with $\omega_j(t)$ at time t , or in general, function of ω and t . Subsequently, the Hilbert amplitude spectrum $H(\omega, t)$ and marginal Hilbert amplitude spectrum $h(\omega)$ over time duration T of the data are defined as

$$H(\omega, t) = \sum_{j=1}^n a_j(t) \quad , \quad h(\omega) = \int_0^T H(\omega, t) dt \quad (6,7)$$

In comparison with Fourier amplitude spectrum in Eq. (2), the Hilbert amplitude spectrum $H(\omega, t)$ provides an extra dimension by including time t in motion frequency and is thus more general than Fourier amplitude spectrum $F(\Omega)$. While the marginal Hilbert amplitude spectrum $h(\omega)$ provides information similar to the Fourier amplitude spectrum, its frequency term is different. Fourier-based frequency (Ω) is constant over the harmonic function persisting through the data window as seen in Eq. (1), while HHT-based frequency ω varies with time based on Eq. (5). As the Fourier transformation window length reduces to zero, the Fourier-based frequency (Ω) approaches the HHT-based frequency (ω). Fourier-based frequency is, however, locally averaged and not truly instantaneous for it depends on window-length, which is controlled by the uncertainty principle and the sampling rate of data.

For recordings that are stationary, the data can typically be decomposed or represented by a series of harmonic functions with time-independent frequency through Fourier-based approach in Eq. (1). If the j -th IMF component, i.e., $C_j(t)$ in Eq. (4), corresponds to a Fourier component with a sine function at a time-independent frequency, the Hilbert transform of the sine function, i.e., $Y_j(t)$ in Eq. (4), can be found to be equal to a cosine function at the same frequency in opposite sign. Because the sign can be changed with a constant phase, the above analysis essentially leads to the consistence between Fourier- and HHT-based approaches in general, and Fourier and marginal Hilbert amplitude spectra in particular, in characterizing linear, stationary phenomena.

For recordings that are nonstationary and results of nonlinear responses such as large-magnitude earthquakes, many studies have showed [e.g., 19] that the marginal Hilbert amplitude spectrum can truthfully represent the nonlinearity-related nonstationary data in comparison with Fourier amplitude spectrum. As a result, an HHT-based approach for characterizing nonlinear site amplification is proposed that is similar to Fourier-based approach. The HHT-based site-amplification factor (FH) is defined

$$FH_s(\Omega) = \sqrt{h_{s,h1}^2 + h_{s,h2}^2} / \sqrt{h_{r,h1}^2 + h_{r,h2}^2} \quad (8)$$

While the above HHT-based site amplification can provide an alternative insight in characterizing and quantifying the site nonlinearity, the role of damping in nonlinear site responses is not discerned from the general features of site nonlinearity, which should be implicitly involved in the factor.

To single out the influences of site damping from the HHT-based site amplification in Eq. (8) that is associated with amplitude $a_j(t)$ in Eqs. (6) and (7), the physical meanings of the j -th IMF component that forms the amplitude $a_j(t)$ in Eq. (4) is first examined below. Since all the IMF components are extracted from acceleration records that are the result of seismic waves generated by a seismic source and propagating in the earth, they should reflect the wave characteristics inherent to the rupture process and the earth medium properties.

Indeed, with the aid of a finite-fault inversion method, signature of the seismic source of the 1994 Northridge earthquake is examined in the large-amplitude IMF components of the ground acceleration recordings [23]. That study only looks over the second to fifth IMF components because they are much larger in amplitude than the remaining higher-order, low-frequency IMF components. The first IMF component was not investigated in the above study because it contains information that is not simply or easily related to the seismic source (e.g., wave scattering in the heterogeneous media). That study shows that the second IMF component is predominantly wave motion generated near the hypocenter, with high-frequency content that might be related to a large stress drop associated with the initiation of the earthquake. As one progresses from the second to the fifth IMF component, there is a general migration of the source region away from the hypocenter with associated longer-period signals as the rupture propagates. In addition, that study shows that some IMF components (e.g., the fifth IMF) can exhibit motion features reflecting the influences of nonlinear site condition.

Because of the relationship of IMF components to the source, Eq. (4) is re-written as

$$X(t) = \Re \sum_{j=1}^n a_j(t) e^{i\theta_j(t)} = \Re \sum_{j=1}^n \Lambda_j(t) e^{-\varphi_j(t) + i\theta_j(t)} \quad , \quad \eta_j(t) = d\varphi_j(t) / dt \quad (9,10)$$

where time-dependent amplitudes $\Lambda_j(t)$ can be interpreted as the source-related intensity, $\varphi_j(t)$ are the exponential factors characterizing the time-dependent decay of the waves in the j -th IMF component due to damping, from which the instantaneous damping factor $\eta_j(t)$ can be defined in Eq. (10) that is similar to the description of the instantaneous frequency in Eq. (5).

With the aid of $a_j(t) = \Lambda_j(t) e^{-\varphi_j(t)}$ in Eq. (9), the Hilbert damping spectrum $D(\omega, t)$ and marginal Hilbert damping spectrum $d(\omega)$ can be found as

$$d(\omega) = \int_0^T D(\omega, t) dt = \sum_{j=1}^n \int_0^T \left[-\frac{\dot{a}_j(t)}{a_j(t)} + \frac{\dot{\Lambda}_j(t)}{\Lambda_j(t)} \right] dt = d^a(\omega) + d^\Lambda(\omega) \quad (11)$$

Equation (11) indicates that the marginal Hilbert damping spectrum consists of two terms: one is from the time-dependent amplitudes $a_j(t)$ that are related to Hilbert and marginal Hilbert amplitude spectra, and the other from source-related intensity, i.e., time-dependent amplitudes $\Lambda_j(t)$.

It is of interest to note that the definition of instantaneous damping factor in Eq. (10) and subsequent spectra in Eq. (11) is different from those in [24-25]. For recordings of impulse-induced or ambient linear vibration responses, some IMF components can be extracted from the data that are related to certain vibration modes [26-28]. Consequently, $\Lambda_j(t)$ are constant and $\eta_j(t)$ are proportional to the damping ratio and damped frequency. The modal damping ratio can then be found. This is essentially the same as those in [24-25], if the latter could prove that $\Lambda_j(t)$ in earthquake recordings is constant and the IMF components are related to certain wave modes.

For recordings to an earthquake, Λ_j is unknown, dependent upon source and time. The influences of Λ_j in the site damping, however, can be removed if two sets of recordings at soil and reference sites are used. Similar to the HHT-based site amplification, the difference of marginal Hilbert damping spectra at soil and reference sites, or named similarly as HHT-based site damping, can eliminate the influences of source that is associated with Λ_j and thus provide the characterization of the site damping. The HHT-based site damping can be found as

$$d_{\Delta}(\omega) = \sqrt{[d_{s,h1}^a(\omega) - d_{r,h1}^a(\omega)]^2 + [d_{s,h2}^a(\omega) - d_{r,h2}^a(\omega)]^2} \quad (12)$$

where use has been made that the source-related damping terms at the soil and referenced sites are approximately equal, i.e., $d_s^{\Lambda}(\omega) \approx d_r^{\Lambda}(\omega)$. Comparing the HHT-based site damping from the mainshock and the aftershock can help quantify the nonlinear site damping.

To illustrate the HHT-based characterization of nonlinearity, the hypothetical record is analyzed again. For comparison with Fourier amplitude spectrum, the marginal Hilbert amplitude spectrum of the recording is also plotted in Fig. 1, showing truthfully the energy distribution of the motion in frequency.

ANALYSIS OF 2001 NISQUALLY EARTHQUAKE RECORDINGS

In this section, the proposed HHT-based approach is used to analyze the recordings of the M6.8 mainshock and the M_L3.4 aftershock of the 2001 Nisqually earthquake at four soft and four stiff soil sites. Recordings at SEW are used as reference-site ones, because SEW has $V_{s30}=433$ m/s that is within the range of V_{s30} values for typical rock sites in the western U.S, which is also used so in Fourier-based studies (e.g., [10]).

Site Amplification

Figure 2a shows the HHT-based site-amplification factors of the mainshock and aftershock at SDS, a soft soil site on artificial fill with nearby liquefaction and the average shear-wave velocity in the top 30m is $V_{s30}=148$ m/s. In calculating the factors (and subsequent HHT-based site amplification and damping), the correction for 1/R geometrical spreading in the recordings at SDS and SEW is not carried out since the hypocentral distances for the sites under investigation are similar. In addition, the marginal amplitude spectra are not smoothed in the calculation, for the non-smoothed spectra more clearly show the characteristics of the HHT-based approach. Examining Fig. 2a shows the following:

- (1) The profile of the HHT-based factor in the frequency band up to 2.5 Hz (referred to as low-frequency range) is generally downshifted in frequency from the aftershock to the mainshock. For example, the profile of the aftershock in 1-2 Hz (1.5-2 Hz in particular) is downshifted to that of the mainshock with an average shift of approximately 0.36 Hz.
- (2) The profile of the HHT-based factor in the frequency band 2.5-7 Hz (intermediate-frequency range) is generally reduced in amplitude from the aftershock to the mainshock. For example, the profile of the aftershock in 3-4 Hz with an averaged-amplitude for the factor 7.26 is reduced to 3.00 for the mainshock, yielding the amplitude-reduction factor of $0.41=3.00/7.26$.
- (3) There is no evidence to support a difference in the factor starting at 7-10 Hz (high-frequency range) between the mainshock and aftershock.

By contrast, the HHT-based factors of the mainshock and aftershock at stiff soil site LAP with $V_{s30}=367$ m/s are shown in Fig. 3a, which demonstrates the following.

- (1) In the low frequency range (below 2.5 Hz), Fig. 3a shows a downshift profile in both frequency and amplitude from the aftershock to mainshock that is similar to Fig. 2a in the low-to-intermediate frequency range, but Fig. 3a shows a smaller frequency downshift (e.g., 0.16 Hz in 1-2 Hz) than the latter (0.36 Hz in 1-2 Hz) in the same frequency band.

- (2) In the intermediate-to-high frequency range, there is almost no difference in the two factors between the mainshock and the aftershock.

With the frequency downshift and amplitude-reduction factor as the measure for the degree of site nonlinearity, comparison of the HHT-based factors at SDS and LAP suggests that SDS has strong site nonlinearity during the mainshock, and LAP has weak site nonlinearity.

To illustrate the characteristics of the HHT-based approach, this study compares the HHT-based site-amplification factors in Figs. 2a and 3a with Fourier-based ones in Fig. 2b and 3b (i.e., Fig. 7 in [10]), revealing the following.

- (1) In the low-frequency range, Fig. 2b shows a frequency-downshift profile from the aftershock to mainshock that is similar to Fig. 2a, but the former shows a smaller shift (about 0.21 Hz) than the latter (about 0.36 Hz) in frequency range 1-2 Hz. Because of the distortion characteristic in Fourier spectral analysis for nonlinearity-related nonstationary data as indicated before, the frequency downshift measured from the HHT-based factors in Fig. 2a may give a more truthful indication of the site nonlinearity than that from the Fourier-based factors in Fig. 2b. In addition, the factors in the low-frequency range in Fig. 2a are generally somewhat larger than those in Fig. 2b.
- (2) In the intermediate-frequency range, Fig. 2b shows an amplitude-reduction profile from the aftershock to mainshock that is similar to Fig. 2a, but Fig. 2b shows a relatively smaller reduction with more oscillation than the latter (e.g., an averaged amplitude-reduction factor of $0.49=1.22/2.48$ in 3-4 Hz for Fig. 2b and $0.41=3.00/7.26$ for Fig. 2a).
- (3) Almost no essential difference is observed from Figs. 3a and 3b in terms of overall profile, amplitude of site-amplification factor, and frequency downshifts between the mainshock and aftershock, except the amplitude change in 1-2 Hz, implying that the two approaches are almost consistent with each other in characterizing and estimating weakly-nonlinear site amplification.

To support the above observations, the site amplifications at three other soft soil sites (i.e., HAR, BOE, and KDK) and three other stiff soil sites (i.e., BHD, THO, and SEU) of the Nisqually earthquake are calculated. Note that all the Fourier spectral ratios are taken from [10]. The results at each and every site are similar to the above. Table 1 summarizes peak ground acceleration, frequency downshift in 1-2 Hz, and amplitude-reduction factor in 3-4 Hz at each site, as well as the averaged value over four soft and four stiff soil sites. The statistical results for nonlinearity characterization are essentially consistent to those at each individual site in Table 1, suggesting that HHT-based approach is equivalent to Fourier-based one in quantifying weakly-nonlinear or linear site amplification, but more effective in quantifying strong site nonlinearity in terms of frequency downshift and amplitude-reduction factor than Fourier-based one.

Site Damping

As an alternative, complementary characterization of site nonlinearity, Figs. 4 and 5 show respectively the HHT-based site damping at soft soil site SDS and stiff soil site LAP. Figure 4 reveals that the site damping at SDS in the mainshock is much larger than that in the aftershock at frequency up to about 5 Hz, suggesting that strong site nonlinearity occurred during the mainshock in the frequency band. The increased damping will decrease the amplified seismic wave responses through the nonlinear soil and thus reduce the site-amplification factor, with the quantities at the linear soil used as a reference. This can be confirmed from Fig. 2a, which shows that the HHT-based factor for site amplification is observably reduced for the mainshock from the aftershock in the similar frequency band of 0.4-7 Hz.

In comparison, Fig. 5 shows that the site damping at LAP is essentially the same between mainshock and aftershock events, suggesting that site LAP is linear or weakly nonlinear for both events. This is consistent with the observations from the site-amplification factors in Figs. 3a,b.

Related Quantifications of Nonlinearity from Site Amplification and Damping

Since Fourier-based approach is not able to estimate appropriately the site damping, particularly for nonlinear sites, Table 1 only lists the damping-increase factors in two frequency bands that are calculated in way similar to amplitude-reduction factor, i.e., the ratio of averaged damping of mainshock over a certain frequency band (i.e., 1-2 and 3-4 Hz) and that of aftershock.

As shown before, the HHT-based site damping is implicitly related to HHT-based site amplification. Therefore, the nonlinearity characterization and quantification from site amplification and damping should bear the relationship, if it is not completely explicit. It is likely difficult in practice to distinguish the influences of different nonlinearity characterization such as frequency downshift, amplitude-reduction factor from site amplification and damping-increase factor from site damping. Nevertheless, we next examine the relationship among the three nonlinearity-characteristics indices from the limited data sets in Table 1.

Table 1 shows that the averaged damping-increase factors for stiff soil site are around unit (1) with 10% variation in both selected frequency bands (1-2 and 3-4 Hz), suggesting that the stiff soil site behaves linearly or weakly nonlinear during the mainshock from the perspective of damping change. This observation is basically consistent with that in terms of frequency downshift and amplitude-reduction factor in the site amplification. Note that the normalization of frequency downshift of 0.16 Hz for the stiff soil site to the center of the frequency band under investigation (i.e., 1.5 Hz of 1-2 Hz) is $10.7\% = 0.16/1.5$, which is marginally within 10% variation.

In contrast, Table 1 shows that the averaged damping-increase factors for the soft soil site are much larger than those in stiff soil site, implying that the soft soil site has strong nonlinear phenomena during the mainshock from the viewpoint of damping change. This fact agrees with the observations from frequency downshift and amplitude-reduction factors from the site amplification. In particular, the increased damping in 3-4 Hz for nonlinear soil will decrease ground motion, thus moderating the site amplification in the same frequency band. In the frequency band 1-2 Hz, the influences of site nonlinearity in the seismic ground motion may combine both effects of frequency downshift due to the loss of shear modulus and decreased amplitude of site-amplification factor due to the increased damping. Therefore, the large averaged frequency downshift of 0.34 for soft soil site is still compatible to the large averaged damping-increase factors of 1.96 in the frequency band of 1-2 Hz in characterizing the site nonlinearity.

Further examination of the damping-increased factors at each individual soft soil site suggests that the variation of the factors is large. In particular, the damping-increase factor at SDS is much larger than those at other sites. This phenomenon is not shown in the frequency downshift and amplitude-reduction factors for the same soft soil sites. This can be explained below.

All the soft soil sites except SDS have no liquefaction nearby. Recordings with liquefaction nearby will not only show the strong nonlinearity features in terms of frequency downshift and amplitude-reduction factors, it will also introduce abnormal, large-amplitude high-frequency spikes. Indeed, the abnormal spikes are observed explicitly in the NS-component of the recording at SDS, but not in the EW-component of SDS and other recordings (see [10]). To have a better understanding of influences of the abnormal spikes in the site damping, we compute the damping-increase factor at SDS in the EW direction only that is 1.84 Hz in 1-2 Hz and 1.75 Hz in 3-4 Hz shown in the parenthesis in Table 1, which are indeed much smaller than those calculated on the basis of two horizontal components of the recording at SDS. This suggests that the abnormal spikes significantly change the characterization of the damping at the site.

While the damping-increase factors in the EW direction at SDS are still larger than those at other sites, again attributable to the strong site nonlinearity with liquefaction nearby, they are comparable with others

since the EW-component of recording at SDS shares the same motion features with others without abnormal spikes. To this end, the NS-component of the recording at SDS can be regarded as a special recording with abnormal signals in this study. While that recording is useful in examining the features of liquefaction, it can be excluded for the statistical study here. To that end, Table 1 provides alternative averaged damping-increase factors with the factors at SDS calculated using two horizontal components replaced by those using the EW-component only. As a viable way, Table 1 also provides the averaged values over three sites excluding SDS. For comparison, the averaged damping-increase factors over three stiff soil sites are also supplied.

It should be noted that the above explanation builds on the limited number of recordings with liquefaction nearby. Therefore, further study is needed along this line.

CONCLUDING REMARKS AND DISCUSSIONS

This study proposes an alternative HHT-based approach in quantifying site nonlinearity and its influences in terms of site amplification and damping. Together with pertinent studies in [29-30], it reveals the following:

1. The HHT-based site-amplification factor is defined as the ratio of marginal Hilbert amplitude spectra, similar to the Fourier-based one that is the ratio of Fourier amplitude spectra. The HHT-based factor has the following distinctive features in comparison with Fourier-based one.
 - (1) The HHT-based factor is essentially equivalent to the Fourier-based one in quantifying linear or weakly-nonlinear site amplification and the changes of characteristics of weak nonlinearity,
 - (2) The HHT-based factor is more effective in quantifying site nonlinearity in terms of frequency downshift in the low-frequency range and amplitude-downshift factor with less oscillation in intermediate-frequency range than Fourier-based one.
 - (3) The HHT-based factor is generally larger than Fourier-based one in low-to-intermediate frequency range for strong site nonlinearity.
1. Instantaneous damping, and Hilbert and marginal Hilbert damping spectra are defined in ways similar to instantaneous frequency, and Hilbert and marginal Hilbert amplitude spectra, respectively. Consequently, the HHT-based site damping is found as the difference of marginal Hilbert damping spectra, which can be used as an alternative index to measure the influences of site nonlinearity in seismic ground responses.
2. Three measurements for characterizing the soil nonlinearity are introduced, i.e., frequency downshift, (spectral ratio) amplitude-reduction factor, and damping-increase factor. The first two are also somewhat implicitly related to the last through a statistical analysis.

ACKNOWLEDGMENTS

The author would like to express his sincere gratitude to Norden E. Huang at NASA, Authur Frankel, and Erdal Safak at USGS, and Lance VanDemark from Colorado School of Mines for providing data, Fourier analysis and results, and more important, constructive suggestions. This work was supported by the National Science Foundation and by US-PRC Researcher Exchange Program administered by Multidisciplinary Center for Earthquake Engineering Research. The opinions, findings and conclusions expressed herein are those of the author and do not necessarily reflect the views of the sponsors.

REFERENCES

1. Kramer SL. "Geotechnical Earthquake Engineering." Prentice-Hall, Inc. Upper Saddle River, NJ, 1996.
2. Frankel A, Mueller C, Barnhard T, Perkins D, Leyendecker E, Dickman N, Hanson S, Hopper M. "USGS national seismic hazard maps," Earthquake Spectra, 2000; 16: 1-19.

3. "NEHRP (National Earthquake Hazards Reduction Program) recommended provisions for seismic regulations for new buildings." Federal Emergency Management Agency Report FEMA 302, Washington DC, 1997, 1-337.
4. Borcherdt, RD. (2002) "Empirical evidence for site coefficients in building code provisions," *Earthquake Spectra*, 2002, 18: 189-217.
5. Hartzell, S. "Variability in nonlinear sediment response during the 1994 Northridge, California, earthquake," *Bull. Seism. Soc. Am.* 1998, 88: 1426-1437.
6. O'Connell, DRH. "Influence of random-correlated crustal velocity fluctuations on the scaling and dispersion of near-source peak ground motions, *Science*, 1999: 283: 2045-2050.
7. Yoshida N, Iai S. "Nonlinear site response and its evaluation and prediction," *The Effects of Surface Geology on Seismic Motion*, (Irikura, Kudo, Okada and Sasatani, eds.), Balkema, Rotterdam, 1998: 71-90.
8. Huang NE, Zheng S, Long SR, Wu MC, Shih HH, Zheng Q, Yen NC, Tung CC, and Liu MH. "The empirical mode decomposition and Hilbert spectrum for nonlinear and nonstationary time series analysis." *Proc. Roy. Soc Lond.*, 1998, A 454 903-995.
9. Vucetic M, Dobry R. "Effect of soil plasticity on cyclic response, *J. Geotech. Eng.*, 1991, 117: 89-107.
10. Frankel AD, Carver DL, Williams RA. "Nonlinear and linear site response and basin effects in Seattle for the M6.8 Nisqually, Washington, Earthquake," *Bull. Seism. Soc. Am.*, 2002, 92: 2090-2109.
11. Field EH, Johnson PA, Beresnev IA, Zeng Y. "Nonlinear ground-motion amplification by sediments during the 1994 Northridge earthquake." *Nature*, 1997, 390: 599-602.
12. Beresnev IA, Field EH, Johnson PA, Van Den Abeele KEA. "Magnitude of nonlinear sediment response in Los Angeles basin during the 1994 Northridge, California, earthquake, *Bull. Seis. Soc. Am.*, 1998, 88: 1097-1084.
13. Joyner WB. "Equivalent-linear ground-response calculations with frequency-dependent damping," *Proceedings of the 31st Joint Meeting of the US-Japan Panel on Wind and Seismic Effects (UJNR)*, Tsukuba, Japan, May 11-14, 1999, 258-264.
14. Bonilla LF, Lavallee D, Archuleta RJ. "Nonlinear site response: laboratory modeling as a constraint for modeling accelerograms." *The Effects of Surface Geology on Seismic Motion*, (Irikura, Kudo, Okada and Sasatani, eds.), Balkema, Rotterdam, 1998.
15. Yound TL et al. "Liquefaction resistance of soils: summary report from the 1996 NCEER and 1998 NCEER/NSF Workshops on evaluation of liquefaction resistance of soil," *ASCE Journal of Geotechnical and Geoenvironmental Engineering*, 1999, 127: 817-833.
16. Safak E. "Models and methods to characterize site amplification from a pair of records," *Earthquake Spectra*, 1997, 13: 97-129.
17. Priestley MB. "Spectral Analysis and Time Series." Vol. 2, *Multivariate Series, Prediction and Control*, Academic Press, London, 1981.
18. Zhang R, Ma S, Safak E, Hartzell S. "Hilbert-Huang transform analysis of dynamic and earthquake motion recordings," *ASCE Journal of Engineering Mechanics*, 2003, 129(8): 861-875.
19. Huang NE, Shen Z, Long RS. "A new view of nonlinear water waves --Hilbert Spectrum." *Ann. Rev. Fluid Mech.* 1999, 31: 417-457.
20. Worden K, Tomlinson GR. *Nonlinearity in Structural Dynamics - Detection, Identification and Modeling*, Institute of Physics Publishing, Bristol and Philadelphia, 2001.
21. Clough RW Penzien J. "Dynamics of Structures." Second Edition, McGraw-Hill, Inc., New York, 1993.
22. Huang NE, Wu ML, Long SR, Shen SP, Wu W, Gloersen P, Fan KL "A confidence limit for the empirical mode decomposition and Hilbert spectral analysis." *Proc. Roy. Soc Lond.*, 2003, A459: 2317-2345.
23. Zhang R, Ma S, Hartzell S. "Signatures of the seismic source in EMD-based characterization of the 1994 Northridge, California, earthquake recordings," *Bulletin of the Seismological Society of America*, 2003, 93(1): 501-518.

24. Salvino LW. "Empirical mode analysis of structural response and damping," Proceedings of 18th International Modal Analysis Conference, Hawaii, USA, February, 2000, 7 p.
25. Loh CH, Wu TC, Huang NE. "Application of the empirical mode decomposition-Hilbert spectrum method to identify near-fault ground-motion characteristics and structural responses," Bull. Seism. Soc. Am. 2001, 91: 1339-1357.
26. Yang JN, Lei Y, Pan S, Huang NE. "System identification of linear structures based on Hilbert-Huang spectral analysis. Part I: Normal modes," Earthquake Engineering and Structural Dynamics, 2002, 32: 1443-1467.
27. Yang JN, Lei Y, Pan S, Huang NE. "System identification of linear structures based on Hilbert-Huang spectral analysis. Part II: Complex modes," Earthquake Engineering and Structural Dynamics, 2002, 32: 1533-1554.
28. Xu YL, Chen SW, Zhang R "Modal identification of Di Wang building under typhoon York using HHT method," The Structural Design of Tall and Special Buildings, 2003, 12(1): 21-47.
29. Zhang R, Hartzell S, Liang J, Hu, YX. "An alternative approach to characterize nonlinear site effects," to appear in Earthquake Spectra, 2004.
30. Zhang R, VanDemark L, Liang J, Hu YX "On estimating site damping with soil nonlinearity from earthquake recordings," to appear in International Journal of Non-Linear Mechanics, 2004.

Table 1: Peak ground acceleration (PGA), frequency downshift in 1-2 Hz, amplitude-reduction factor in 3-4 Hz, and damping-increase factor in 1-2 and 3-4 Hz for soft and stiff soil sites. The numbers in parenthesis of SDS indicate that the damping-increase factors are calculated for the EW-component only, not the two horizontal components.

Sites	PGA of Mainshock (g)		Freq.-Downshift(Hz) (1-2 Hz)		Ampl.-Reduction Factor (3-4 Hz)		Damping-Increase Factor (HHT only)	
	NS	EW	HHT	Fourier	HHT	Fourier	(1-2 Hz)	(3-4 Hz)
Soft Soil								
BOE	0.19	0.19	0.33	0.15	0.34	0.54	1.27	1.02
HAR	0.22	0.19	0.34	0.24	0.29	0.32	1.2	1.01
KDK	0.19	0.15	0.33	0.13	0.87	1.03	1.55	0.88
SDS	0.29	0.22	0.36	0.21	0.41	0.49	3.8(1.84)	3.39(1.75)
AVERAGE	0.22	0.19	0.34	0.18	0.48	0.60	1.96(1.47)	1.57(1.17)
(AVERAGE OVER BOE, HAR and KDK)							1.34	0.97
Stiff Soil								
BHD	0.15	0.17	0.19	0.25	1.14	0.98	1.31	1.2
LAP	0.10	0.09	0.16	0.15	0.99	1.02	1.11	1.12
SEU	0.10	0.10	0.12	0.10	1.01	1.01	0.95	1.06
THO	0.09	0.12	0.18	0.15	0.75	1.04	0.7	1.03
AVERAGE	0.11	0.12	0.16	0.16	0.97	1.01	1.02	1.10
(AVERAGE OVER BHD, LAP and SEU)							1.12	1.13

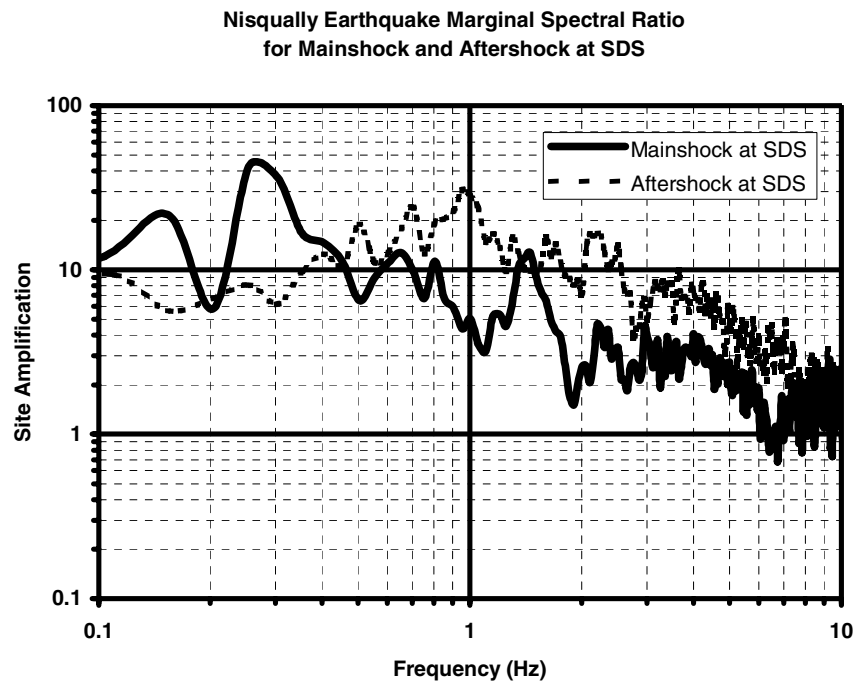


Figure 2a: HHT-based site amplification at soft soil site SDS for mainshock and aftershock of the 2001 Nisqually earthquake.

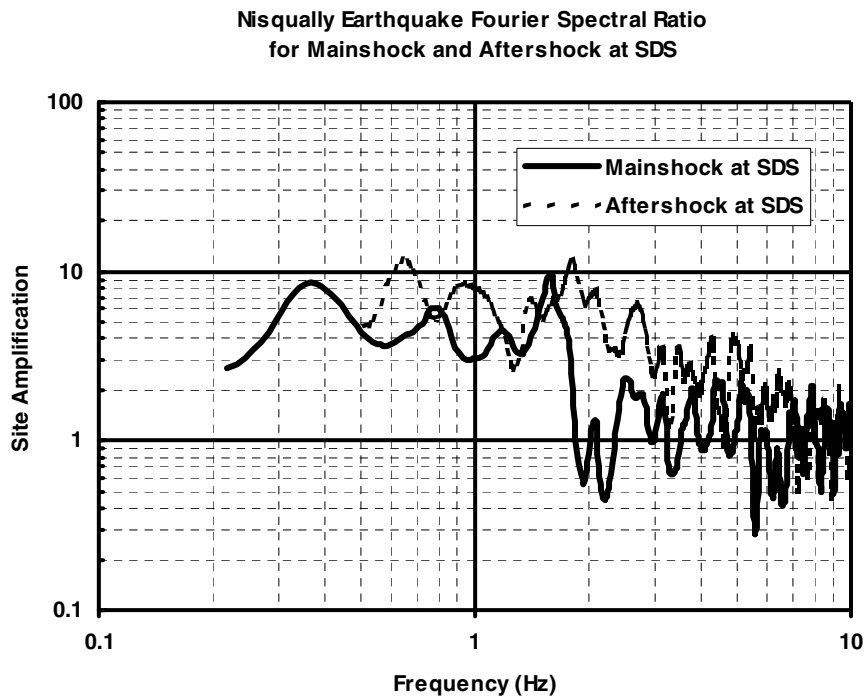


Figure 2b: Fourier-based site amplification at soft soil site SDS for mainshock and aftershock of the 2001 Nisqually earthquake.

Nisqually Earthquake Marginal Spectral Ratio
for Mainshock and Aftershock at LAP

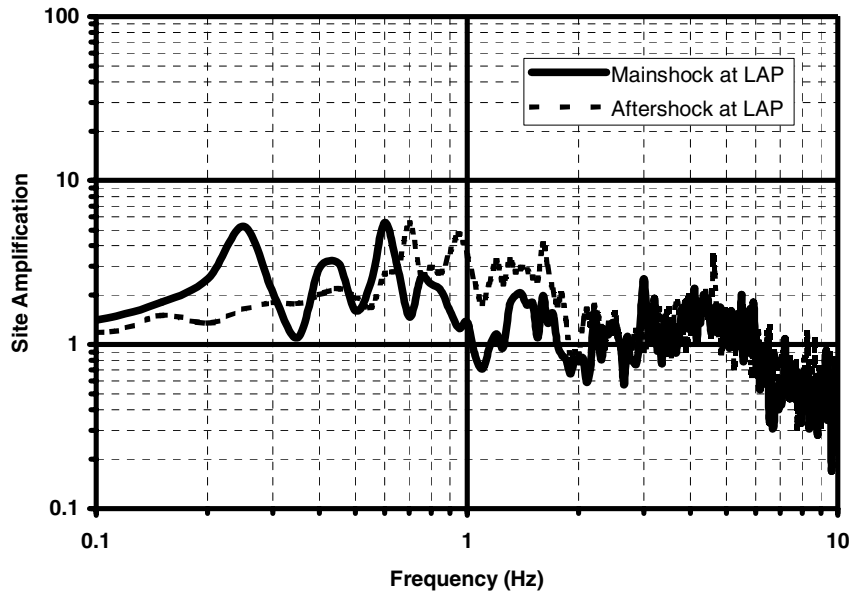


Figure 3a: HHT-based site amplification at stiff soil site LAP for mainshock and aftershock of the 2001 Nisqually earthquake.

Nisqually Earthquake Fourier Spectral Ratio
for Mainshock and Aftershock at LAP

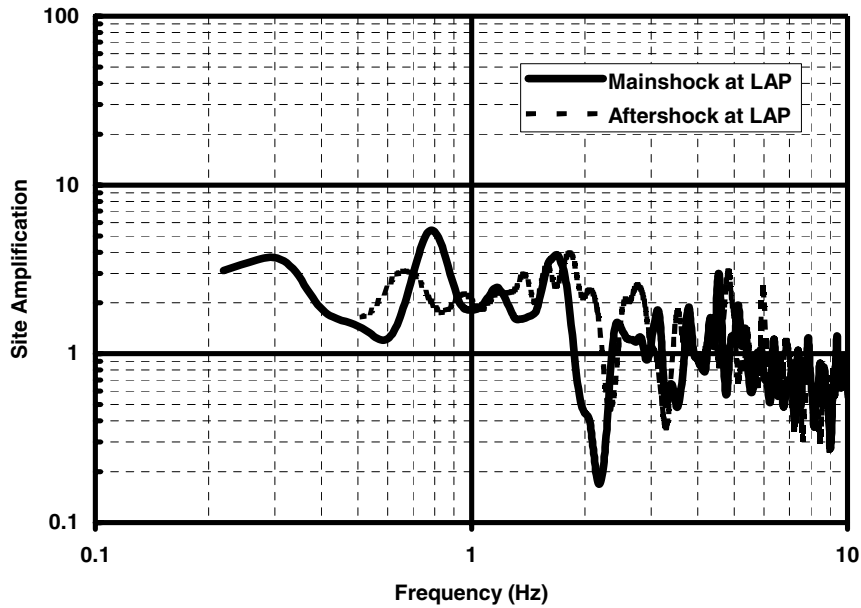


Figure 3b: Fourier-based site amplification at stiff soil site LAP for mainshock and aftershock of the 2001 Nisqually earthquake.

Nisqually Earthquake Marginal Damping Difference
for Mainshock and Aftershock at SDS, a Soft Soil Site

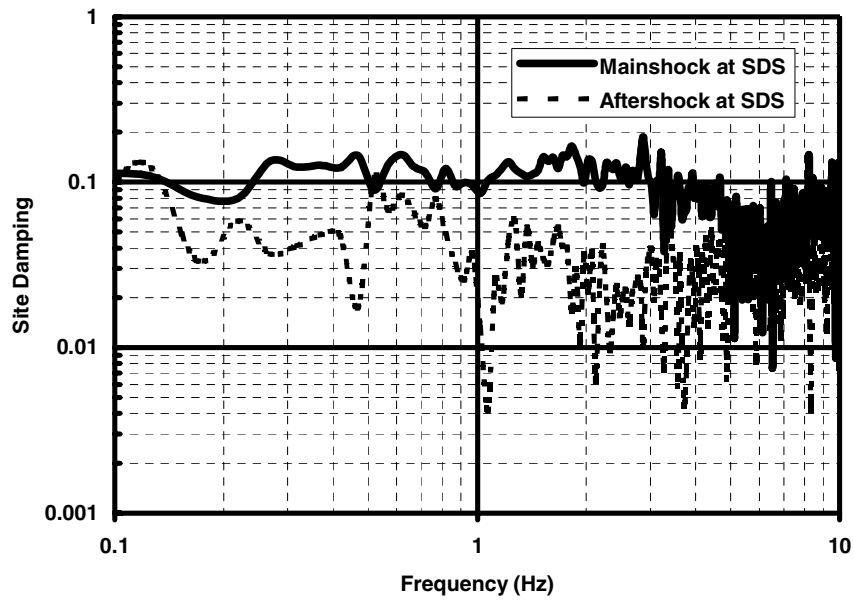


Figure 4: Site damping at soft soil site SDS for mainshock and aftershock of the 2001 Nisqually earthquake.

Nisqually Earthquake Marginal Damping Difference
for Mainshock and Aftershock at LAP, a Stiff Soil Site

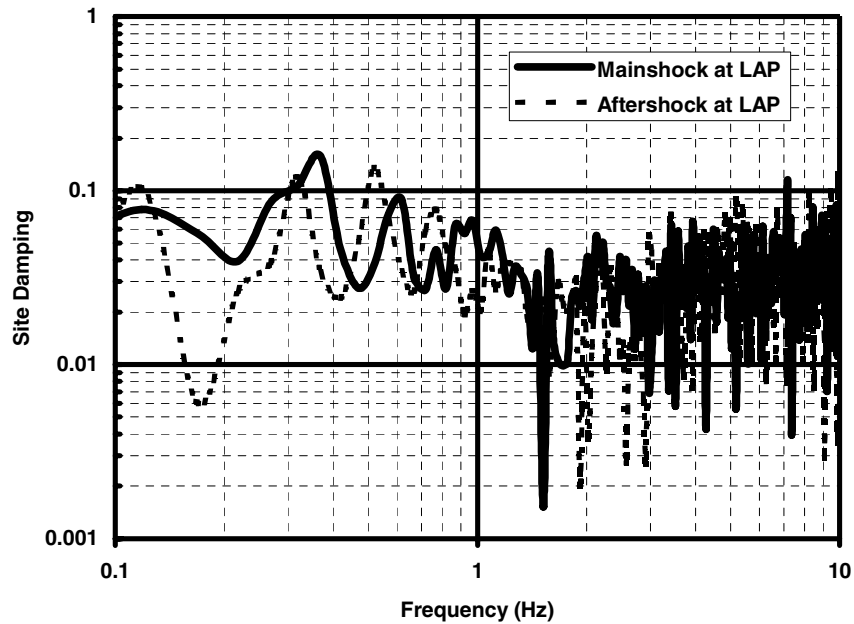


Figure 5: Site damping at stiff soil site LAP for mainshock and aftershock of the 2001 Nisqually earthquake.